ADVANCES IN COLLOID AND INTERFACE SCIENCE
Elsevier Publishing Company, Amsterdam – Printed in the Netherlands

Light Scattering from Liquid Interfaces

A. VRIJ

van 't Hoff Laboratory, State University of Utrecht, Utrecht (The Netherlands)

CONTENTS

1. Introduction 40
2. Theory for a single interface 42
   2.1. Statistical analysis of corrugations 42
   2.2. Amplitude of scattered light 43
   2.3. Intensity of the scattered light 46
3. Light scattering equations for a single interface 46
   3.1. Interface between two transparent liquids 47
   3.2. Interface between a transparent liquid (1) and a totally-reflecting liquid (2) . . . 49
4. Experiments on single interfaces 49
   4.1. Air–mercury interface 49
   4.2. Surface of transparent liquids 53
   4.3. Water surfaces covered with films 55
   4.4. Interfaces near the critical point 56
5. Thin liquid films 57
   5.1. Theory 57
   5.2. Experiments 60
   5.3. Interaction between the film surfaces 62
Acknowledgement 63
References 63

1. Introduction

The interface between a liquid and its vapor or the interface between two immiscible liquids is not perfectly flat, but more or less rough. This roughness can be demonstrated by throwing an intense light beam on the liquid interface; most of the incident light is reflected and refracted, but also a very small part of it is scattered (diffusely reflected) in all directions. This surface light scattering or surface opalescence is caused by the roughness of the surface or interface. The roughness is caused by thermal motion.

The phenomenon was predicted by von Smoluchowski[1] in 1908. He stated that the light scattering from the liquid–vapor interface, in addition to the more familiar light scattering of the bulk of the liquid, would be observable near the critical point where the surface tension of the liquid is low and the corrugations are easily formed.

A quantitative theory was developed by Mandelstam[2] in 1913. He described the thermal roughness of the liquid interface as a spectrum of "waves" and was able to calculate the mean square amplitude of the "waves" as a function of wavelength, assuming that their creation is counteracted by interfacial tension and gravity. The surface opalescence in a certain direction is proportional to the mean square amplitude of the corresponding interface "wave", the wavelength of which is simply related to the wavelength of the incident light and the angles of incidence and observation. Mandelstam found that the intensity is proportional to the factor $(n^2 - 1)^2\,(kT/\lambda^2\gamma)$, (where k = Boltzmann's constant; T = absolute temperature; λ = wavelength of the incident light; γ the interfacial tension and n = ratio of refractive indices of the two media bounded by the interface) and depends strongly upon the angles. The opalescence rises steeply when approaching the reflected or the refracted beam. Its magnitude is quite low: at 15°, from the reflected beam the scattering from 1 cm^2 of a clean water surface is about the same as the scattering from 1 cm^3 of its bulk.

Mandelstam also performed some visual observations on the light scattering from a carbon disulfide–methanol interface near the critical solution temperature. The surface scattering could be distinguished clearly from the (also large) bulk scattering. Its intensity increased sharply with increase in temperature up to the critical mixing temperature and also when approaching the reflected beam, in agreement with theory.

He also observed that the scattered light was polarised. Very near the critical point the reflected beam vanished.

The scope of the subject was extended considerably by Raman and Ramdas[3–9] who showed that the phenomenon is not confined to the vicinity of the critical point, but is shown by all liquid surfaces, even when far below the critical point.

They performed measurements on the liquid–vapor interface of some 60 transparent liquids and on mercury. The results were in fair agreement with Mandelstam's theory and with extended versions of it developed by Gans[10,11] and Andronov and Leontovicz[12], who also considered the scattering outside the plane of incidence. The angle dependence, however, deviated from the theory.

Further papers[13–16] on the subject are scarce and the phenomenon has not attracted attention, as far as we know, since 1942. This may be due to several causes. The surface light scattering has a small intensity; it usually cannot be observed independently of the accompanying bulk light scattering. Dust and other contaminations disturb the measurement, and, finally, the most interesting physico-chemical quantity that can be found from the theory given so far is the surface or interfacial tension γ, for the measurement of which many other, more convenient, methods are available.

We are nevertheless of the opinion that the subject deserves more attention than has hitherto been devoted to it. If developed further, it may become a valuable tool in the surface chemistry of liquid interfaces.

Because the light scattering is inversely proportional to the interfacial tension, it may be used in cases where interfacial tensions are exceptionally low (coacervates, spontaneous emulsification) where more conventional methods may fail.

Further, liquid interfaces covered with mono- or polymolecular films may be studied. Interfaces that are not in equilibrium (*e.g.* through interfacial diffusion of a solute component) are also possible objects; light scattering would be a sensitive tool to observe their instability.

The intensity, the state of polarization, the angle- and wavelength dependence of the scattered light offer a great variety of parameters that can be measured much more precisely with modern optical and electronic equipment than was possible some forty years ago.

It should be possible to study the *dynamics* of the corrugations if one is able to measure the *spectrum* of the scattered light. When very pure monochromatic incident light is used, the light scattered by the interface will no longer be purely monochromatic. When for example the corrugations are travelling "waves", the spectrum of the scattered light would show, because of the Doppler effect, two peaks at frequencies symmetrically positioned around the frequency of the incident light. The frequency-shift would be proportional to the velocity of the travelling "wave" and the width of the peaks would be a measure of its damping. If, however, the "corrugations are not travelling, but are stationary "waves", the spectrum of the scattered light would show only a broadened peak at the frequency of the incident light.

Recently, the light scattering spectrum of (bulk) liquids and a polymer solution was analysed in this way by making use of a laser as a light source combined with a Fabry–Perot etalon or with an optical heterodyne detector[17–20]. The velocity of the (hypersonic) thermal sound waves in the liquids and the diffusion coefficient of the polymer could be obtained.

The author has recently[21] extended the theory and the experiments to thin free liquid films (as found in soap bubbles). It was found that the light scattering not only depends on the surface tension of the film but also on the intermolecular forces (*e.g.* electrostatic repulsion and van der Waals attraction) present in the film.

In this paper both the older work on single liquid–liquid interfaces and the more recent work on thin liquid films will be reviewed. Section 2 contains an outline of the theory for single liquid interfaces, and a list of equations is given in Section 3. In Section 4 the older experiments are reviewed and in Section 5 the work on thin films.

2. Theory for a single interface

The calculation of the light scattering from a rough (or corrugated) interface is performed in two steps. The first step involves a statistical analysis of the corrugations in the interface caused by thermal motion whilst the second involves a calculation of the disturbance of the primary incident light wave by these corrugations.

2.1 STATISTICAL ANALYSIS OF CORRUGATIONS

The statistical analysis of the interface corrugations, first developed by Mandelstam and accepted by all subsequent authors, is performed as follows. The mean position of the interface is taken in the X–Y plane of a rectangular coordinate system and the deviation from this mean position (in the Z-direction) is defined by a function $\zeta = \zeta(x,y)$. It is assumed that the thickness of the interface is small with respect to the wavelength of the light used and that the liquids are incompressible.

The function $\zeta(x,y)$ is expanded in a Fourier series[12] in a square with length a ($-a/2<x<a/2$; $-a/2<y<a/2$). ($a \gg \lambda$, where λ is the wavelength of the light).

$$\zeta = \sum_{\varrho=-\infty}^{+\infty} \sum_{\sigma=-\infty}^{+\infty} \zeta_{\varrho\sigma}\, e^{ip(\varrho x + \sigma y)} \tag{2.1}$$

Here $p = 2\pi/a$ and the $\zeta_{\varrho\sigma}$'s are the (complex) Fourier coefficients. Since ζ is real, the coefficients are connected in pairs by the relations

$$\zeta_{-\varrho,-\sigma} = \zeta^*_{\varrho,\sigma}; \quad \zeta_{\varrho,-\sigma} = \zeta^*_{-\varrho,\sigma}; \quad \zeta_{-\varrho,\sigma} = \zeta^*_{\varrho,-\sigma}$$

where $\zeta^*_{\varrho\sigma}$ is the complex conjugate of $\zeta_{\varrho\sigma}$, etc.

The wavelengths of the modes are given by:

$$\Lambda = a(\varrho^2 + \sigma^2)^{-\frac{1}{2}} \tag{2.2}$$

Now it turns out (see next section) that the intensity of the light scattered by a certain mode is proportional to the mean square amplitude of that mode; it thus suffices to characterize the roughness of the interface by the numbers $\overline{\zeta_{\varrho\sigma}\zeta^*_{\varrho\sigma}}$, where the bar signifies a time average. Mandelstam calculated these averages by making use of the equipartition principle which states that the work necessary to create each mode is equal to $kT/2$. Consideration of "macroscopic" forces in the calculation of the work (or free energy) suffices because only modes

with wavelengths of the order of the wavelength of visible light contribute significantly to the light scattering. Two types of forces are considered: capillary and gravity forces.

The work to create a corrugation at constant temperature is

$$\Delta F = \Delta F_1 + \Delta F_2 \tag{2.3}$$

where ΔF_1 is equal to:

$$\Delta F_1 = \gamma \Delta O \tag{2.4}$$

γ is the interfacial tension and ΔO is the increase of the area of the interface. Because of the smallness of the amplitude of the corrugations this transforms into:

$$\Delta F_1 = \tfrac{1}{2}\gamma \int_{-\frac{1}{2}a}^{+\frac{1}{2}a} \int \left[\left(\frac{\delta \zeta}{\delta x} \right)^2 + \left(\frac{\delta \zeta}{\delta y} \right)^2 \right] dx\, dy \tag{2.5}$$

ΔF_2, which is due to gravity, can be written as follows:

$$\Delta F_2 = \tfrac{1}{2}\mu g \int_{-\frac{1}{2}a}^{+\frac{1}{2}a} \int [\zeta(x, y)]^2\, dx\, dy \tag{2.6}$$

Here μ is the density difference between the two liquids separated by the interface and g the gravity constant. Substituting eqn. (2.1) into the eqns. (2.5) and (2.6), and applying the equipartition principle then yields:

$$\overline{\zeta_{\varrho\sigma}\zeta^*_{\varrho\sigma}} \left[\tfrac{1}{2}\gamma a^2 p^2 (\varrho^2 + \sigma^2) + \tfrac{1}{2}\mu g a^2 \right] = \tfrac{1}{2} kT \tag{2.7}$$

or

$$\overline{\zeta_{\varrho\sigma}\zeta^*_{\varrho\sigma}} = \frac{kT/a^2}{\gamma p^2 (\varrho^2 + \sigma^2) + \mu g} \tag{2.8}$$

or

$$\overline{\zeta_{\varrho\sigma}\zeta^*_{\varrho\sigma}} = \frac{kT/a^2}{(4\pi^2\gamma/\Lambda^2) + \mu g} \tag{2.9}$$

The contribution of gravity can be neglected when $\gamma \gg \mu g \Lambda^2/4\pi^2$ or $\gamma \gg 6\mu \times 10^{-8}$ dynes/cm^2 (*i.e.* $\Lambda \simeq \lambda \simeq 5 \times 10^{-5}$ cm; g $\simeq 10^3$ cm sec^{-2}) and this is in practice always the case.

Then eqns. (2.8) and (2.9) become:

$$\overline{\zeta_{\varrho\sigma}\zeta^*_{\varrho\sigma}} = \frac{kT}{\gamma p^2 a^2 (\varrho^2 + \sigma^2)} = \frac{kT\Lambda^2}{4\pi^2\gamma a^2} \tag{2.10}$$

Eqn. (2.10) will be employed in the calculation of the light scattering intensity.

2.2 AMPLITUDE OF SCATTERED LIGHT

The problem is to calculate the light scattered when a plane electromagnetic wave falls on an interface separating two media with a different refractive index and containing corrugations as given by eqn. (2.1), using Maxwell's equations.

Because these equations are linear, the total scattering will be a linear superposition of the scattering given by each mode.

A large variety of solutions for this problem, depending on the amplitudes and wavelengths of the modes and the refractive indices of the materials, are discussed by Beckmann and Spizzichino[22]. In our case ζ is always much smaller than Λ and the solutions given by Rayleigh[23], Mandelstam, Andronov and Leontovicz, and Gans are appropriate. Rayleigh found that if the illuminated surface area is much larger than λ^2, the scattering degenerates into a spectrum of diffracted waves, the directions of which are given by elementary diffraction theory. If the incident light travels from medium 1 (with refractive index n_1) into medium 2 (with refractive index n_2) the directions are given by:

$$\begin{aligned} \sin\theta\cos\varphi - \sin\theta_0 &= \varrho p/k_1 \\ \sin\theta\sin\varphi &= \sigma p/k_1 \end{aligned} \tag{2.11}$$

for waves diffracted into medium 1, and

$$\begin{aligned} \sin\theta'\cos\varphi' - \sin\theta_0' &= \varrho p/k_2 \\ \sin\theta'\sin\varphi' &= \sigma p/k_2 \end{aligned} \tag{2.12}$$

for waves diffracted into medium 2. Here $k_1 = 2\pi/\lambda_1$ and $k_2 = 2\pi/\lambda_2$; λ_1 and λ_2 are the wavelengths of the light in medium 1 and 2, respectively; θ_0 and θ_0' are the angles of incidence and refraction of the primary beam (lying in the XZ-plane), whilst θ, θ' and φ, φ' define the altitude and azimuth of the diffracted waves in medium 1 and 2, respectively (see Fig. 1).

Further, Snell's law applies:

$$\varphi = \varphi'; \quad \sin\theta/\sin\theta' = k_2/k_1 \equiv n_2/n_1 = n \tag{2.13}$$

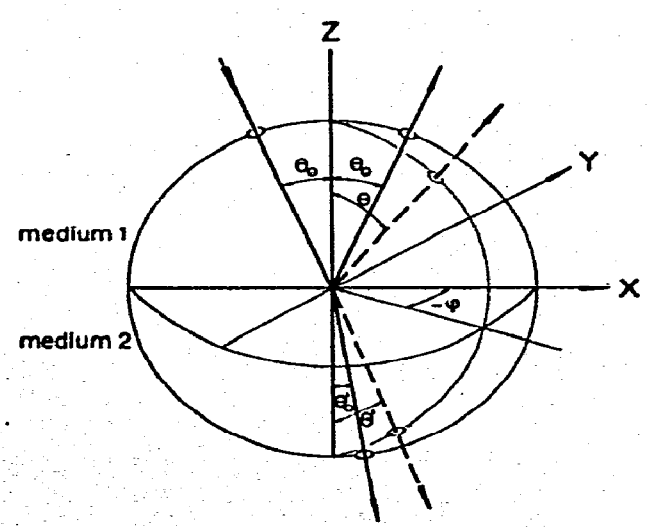

Fig. 1. Incident, reflected and refracted beams (———); diffracted beams (— — —).

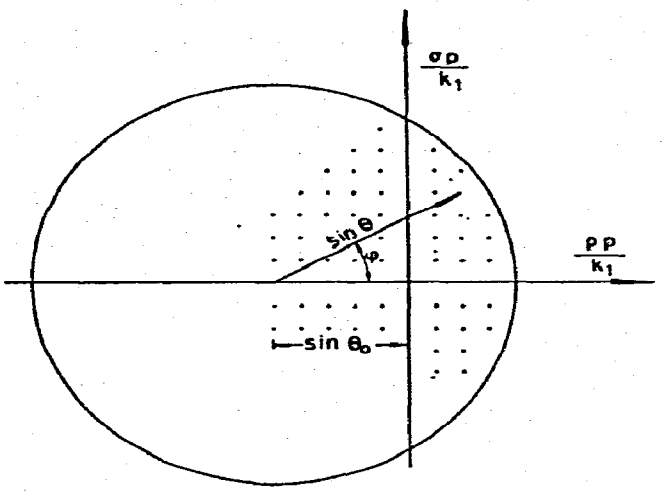

Fig. 2. Relation between the angles of incidence, θ_0 and observation, θ, φ, and the Fourier indices ϱ and σ [see eqn. (2.11)].

Relation (2.11) is illustrated in Fig. 2. For each pair of values (ϱ,σ) the direction of the diffracted wave (θ,φ), at a certain θ_0, can be read from this figure. Because $\zeta_{\varrho,\sigma} \ll \lambda$, only the first-order spectra contribute significantly and each (complex) mode $\zeta_{\varrho\sigma}\, e^{ip(\varrho x + \sigma y)}$ gives two diffracted waves, the directions of which are given by eqns. (2.11) and (2.12). Modes with values of ϱ and σ falling outside the circle of unit radius in Fig. 2 do not contribute to the light scattering in this approximation.

For an incident light wave with unit amplitude and with the electrical vector perpendicular to the plane of incidence, the amplitude of the diffracted wave becomes[2,12,21]:

$$A_{\varrho\sigma} = 2ik_1\zeta_{\varrho\sigma}\,\frac{\sin(\theta_0 - \theta_0')\cos\theta_0 \sin\theta\cos\varphi}{\sin(\theta + \theta')} \tag{2.14}$$

which may be transformed into[21]

$$A_{\varrho\sigma} = \frac{ik_1\zeta_{\varrho\sigma}}{2\cos\theta}(n^2 - 1)\, t_s(1)\, t_{os}(1)\cos\varphi \tag{2.15}$$

where $t_s(1)$ and $t_{os}(1)$ are Fresnel transmission coefficients and n is defined in eqn. (2.13)

$$t_{os}(1) = \frac{2\cos\theta_0}{\cos\theta_0 + n\cos\theta_0'} \tag{2.16}$$

$$t_s(1) = \frac{2\cos\theta}{\cos\theta + n\cos\theta'} \tag{2.17}$$

The intensity of the scattered light is proportional to $|A_{\varrho\sigma}|^2$. Equations for other states of polarization are given in section 3.

2.3 INTENSITY OF THE SCATTERED LIGHT

The intensity of the scattered light is conveniently expressed by a dimensionless quantity, S, called the "surface scattering ratio" and defined as the energy flow scattered per unit of *interface* area and per unit of solid angle divided by the energy flow per unit of *wavefront* area of the incident wave.

The energy flow per unit of wavefront area of the diffracted wave (ϱ,σ), divided by the energy flow per unit of wavefront area of the incident wave is given by

$$I_{\varrho\sigma}/I_0 = |A_{\varrho\sigma}|^2 \tag{2.18}$$

Then the energy flow of all the diffracted waves falling into a solid angle $d\Omega$ (in medium 1; $z > 0$) per unit of *interface* area is:

$$I_0|A_{\varrho\sigma}|^2 \cos\theta\, \Delta\varrho\Delta\sigma \tag{2.19}$$

where $\Delta\varrho\Delta\sigma$, the number of modes contributing to the light scattered into $d\Omega$, is equal to (see Fig. 2):

$$\Delta\varrho\Delta\sigma = (a/\lambda_1)^2 \cos\theta \sin\theta\, d\theta d\varphi = (a/\lambda_1)^2 \cos\theta\, d\Omega \tag{2.20}$$

Then S becomes

$$S(\theta_0, \theta, \varphi) = \overline{|A_{\varrho\sigma}|^2}\, (a/\lambda_1)^2 \cos^2\theta \tag{2.21}$$

Because $a \gg \lambda_1$, many modes will diffract into a (not too small) solid angle $d\Omega$ and the scattered light will be diffuse. Combining eqns. (2.21), (2.15) and (2.10), and using eqn. (2.11) to transform $(\varrho^2 + \sigma^2)$, yields:

$$S = \frac{\frac{1}{4}(kT/\lambda_1^2)\,(n^2 - 1)^2\, t_s^2(1)\, t_{0s}^2(1) \cos^2\varphi}{\gamma(\sin^2\theta_0 + \sin^2\theta - 2\sin\theta_0 \sin\theta \cos\varphi} \tag{2.22}$$

For $\varphi \simeq 0$ this reduces to

$$S = \frac{\frac{1}{4}\,(kT/\lambda_1^2)\,(n^2 - 1)^2\, t_s^2(1)\, t_{0s}^2(1)}{\gamma(\sin\theta_0 - \sin\theta)^2} \tag{2.23}$$

Eqn. (2.23) — here written in a somewhat different form — was first obtained by Mandelstam. It applies for light scattered in the "reflection half plane" and for incident light with the electrical vector perpendicular to the plane of incidence.

Equations for other states of polarization are much more complicated, and are listed in the following section.

3. Light scattering equations for a single interface

In this section, equations for the intensity and state of polarization of the scattered light are listed for an interface between two transparent liquids and for an interface between a transparent and a totally-reflecting liquid. The equations

are due to Gans[10,11] and Andronov and Leontovicz[12], but are written here more compactly by introducing the following coefficients:

$$t_{os}(1) = \frac{2\cos\theta_o}{\cos\theta_o + n\cos\theta_o'}; \qquad t_{op}(1) = \frac{2\cos\theta_o}{n\cos\theta_o + \cos\theta_o'} \tag{3.1}$$

$$t_s(1) = \frac{2\cos\theta}{\cos\theta + n\cos\theta'}; \qquad t_p(1) = \frac{2\cos\theta}{n\cos\theta + \cos\theta'} \tag{3.2}$$

$$t_s(2) = \frac{2n\cos\theta'}{\cos\theta + n\cos\theta'}; \qquad t_p(2) = \frac{2n\cos\theta'}{n\cos\theta + \cos\theta'} \tag{3.3}$$

(These are known as Fresnel transmission coefficients for the electrical component[24])

$$n = n_2/n_1 \tag{3.4}$$

$$H = \tfrac{1}{4}(kT/\lambda_1^2\gamma)\,(n^2 - 1)^2\,(\sin^2\theta_o + \sin^2\theta - 2\sin\theta_o\sin\theta\cos\varphi)^{-1} \tag{3.5}$$

$$H' = \tfrac{1}{4}(kT/\lambda_1^2\gamma)\,(\sin^2\theta_o + \sin^2\theta - 2\sin\theta_o\sin\theta\cos\varphi)^{-1} \tag{3.6}$$

3.1 INTERFACE BETWEEN TWO TRANSPARENT LIQUIDS

Gans considered four cases (the incident light always travels from medium 1 to medium 2 in the XY-plane):

- (I_a) incident electrical component is polarized perpendicular to the plane of incidence with $\sin\theta_o < n$;
- (I_b) as I_a but with $\sin\theta_o > n$ (total reflection of incident light);
- (II_a) incident electrical component is polarized parallel to plane of incidence with $\sin\theta_o < n$;
- (II_b) as II_a but with $\sin\theta_o > n$.

Case I_a

Scattering observed in medium 1 ($z > 0$):

$$S(1) = Ht_{os}^2(1)[t_s^2(1)\cos^2\varphi + t_p^2(1)\cos^2\theta'\sin^2\varphi] \tag{3.7}$$

The polarization angle, μ_1, (with the horizontal in the point of observation) is given by:

$$\tan\mu_1 = -[t_p(1)/t_s(1)]\cos\theta'\tan\varphi \tag{3.8}$$

Scattering observed in medium 2 ($z < 0$):

$$S(2) = nHt_{os}^2(1)[t_s^2(2)\cos^2\varphi + t_p^2(2)\cos^2\theta\sin^2\varphi] \tag{3.9}$$

[Eqn. (3.5) for H also applies for $z < 0$, although the observation angles are θ' and φ].

The polarization angle is given by:

$$\tan \mu_2 = -[t_p(2)/t_s(2)]\cos\theta \tan\varphi \tag{3.10}$$

Case I_b

For this case ($\sin\theta_o > n$), θ_o' and thus $t_{os}(1)$ are complex. The same formulae apply as in case I_a, but with $t_{os}^2(1)$ replaced by $|t_{os}(1)|^2 = 4\cos^2\theta_o/(1 - n^2)$. The equations for $\tan\mu_1$ and $\tan\mu_2$ are not changed; the light remains linearly polarized.

Case II_a

Scattering observed in medium 1 ($z > 0$):

$$S(1) = Ht_{op}^2(1)\,[t_s^2(1)\cos^2\theta_o' \sin^2\varphi + t_p^2(1)(\sin\theta \sin\theta_o - \cos\theta' \cos\theta_o' \cos\varphi)^2] \tag{3.11}$$

$$\tan\mu_1 = \frac{[t_p(1)/t_s(1)]\,[\cos\theta' \cos\theta_o' \cos\varphi - \sin\theta \sin\theta_o]}{\cos\theta_o' \sin\varphi} \tag{3.12}$$

Scattering observed in medium 2 ($z < 0$):

$$S(2) = nHt_{op}^2(1)[t_s^2(2)\cos^2\theta_o' \sin^2\varphi + t_p^2(2)(\sin\theta \sin\theta_o' + \cos\theta \cos\theta_o' \cos\varphi)^2] \tag{3.13}$$

$$\tan\mu_2 = -\frac{[t_p(2)/t_s(2)]\,[\cos\theta \cos\theta_o' \cos\varphi + \sin\theta \sin\theta_o']}{\cos\theta_o' \sin\varphi} \tag{3.14}$$

Case II_b

For this case ($\sin\theta_o > n$),

$t_{op}^2(1)$ has to be replaced by $|t_{op}(1)|^2$;

$\cos^2\theta_o'$ by $(\sin^2\theta_o/n^2) - 1$;

$(\sin\theta \sin\theta_o - \cos\theta' \cos\theta_o' \cos\varphi)^2$ by $|[\sin\theta \sin\theta_o - (i/n)\cos\theta' (\sin^2\theta_o - n^2) \cos\varphi]|^2$;

and

$(\sin\theta \sin\theta_o' + \cos\theta \cos\theta_o' \cos\varphi)^2$ by $|[\sin\theta(\sin\theta_o/n) + (i/n) \cos\theta (\sin^2\theta_o - n^2) \cos\varphi]|^2$.

The values of $\tan\mu_1$ and $\tan\mu_2$ are complex; the light is elliptically polarized.

Scattering observed in medium 1 ($z > 0$):

$$S(1) = H\left[\frac{4\cos^2\theta_o}{n^4\cos^2\theta_o + \sin^2\theta_o - n^2}\right]\Big\{t_s^2(1)\sin^2\varphi\,(\sin^2\theta_o - n^2) + t_p^2(1)\,[n^2\sin^2\theta_o \sin^2\theta + (\sin^2\theta_o - n^2)\cos^2\theta' \cos^2\varphi]\Big\} \tag{3.15}$$

Scattering observed in medium 2 ($z < 0$):

$$S(2) = nH\left[\frac{4\cos^2\theta_o}{n^4\cos^2\theta_o + \sin^2\theta_o - n^2}\right]\Big\{t_s^2(2)\sin^2\varphi\,(\sin^2\theta_o - n^2) + t_p^2(2)\,[\sin^2\theta_o \sin^2\theta + (\sin^2\theta_o - n^2)\cos^2\theta \cos^2\varphi]\Big\} \tag{3.16}$$

Gans did not mention explicitly the cases where $\sin\theta > n$, or $\sin\theta' > 1/n$. It is clear, however, that then θ', respectively θ, are complex, and similar substitutes as given in case I_b and II_b for all factors containing θ', respectively θ, have to be made.

3.2 INTERFACE BETWEEN A TRANSPARENT LIQUID (1) AND A TOTALLY REFLECTING LIQUID (2)

The formulae of section 3.1 apply but with $n = \infty$ and $\theta_0' = \theta' = 0$ $(z > 0)$. There are 2 cases:

(I) incident electrical component is polarized *perpendicular* to plane of incidence

(II) incident electrical component is polarized *parallel* to plane of incidence.

Case I

Scattering observed in medium 1 $(z > 0)$:

$$S(1) = 16H' \cos^2\theta_0 (\cos^2\theta \cos^2\varphi + \sin^2\varphi) \tag{3.17}$$

$$\tan\mu_1 = -\tan\varphi/\cos\theta \tag{3.18}$$

Case II

Scattering observed in medium 1 $(z > 0)$:

$$S(1) = 16H' [\cos^2\theta \sin^2\varphi + (\sin\theta \sin\theta_0 - \cos\varphi)^2] \tag{3.19}$$

$$\tan\mu_1 = (\cos\varphi - \sin\theta \sin\theta_0)/\cos\theta \sin\varphi \tag{3.20}$$

4. Experiments on single interfaces

4.1 AIR-MERCURY INTERFACE

Raman and Ramdas[4] performed experiments on the air–mercury interface. A clean mercury surface was obtained as follows. Purified mercury was transferred into a distillation apparatus consisting of two fairly large glass bulbs, connected by a thoroughly cleaned glass tube. The mercury was transferred to bulb 1, partially distilled over to bulb 2, and then shaken back to bulb 1, so that the dust and impurities were concentrated in bulb 1 whereas mercury with a perfectly clean surface was obtained in bulb 2. The procedure was repeated 6 times.

Sunlight was concentrated by an achromatic lens upon the metallic surface in the glass bulb. The outside of the bulb was partially painted black to obtain a dark background for observation. The focal spot was distinctly visible and showed a *bluish-white* opalescence. It was perfectly structureless, uniform and continuous

when examined through a microscope. The intensity and state of polarization were determined at several angles of incidence and observation.

4.1.1 Normal incidence of unpolarized light ($\theta_0 = 0$)

The intensity of the surface opalescence was measured at $\theta = 45°$ by photographic photometry and compared with the intensity from a smooth surface of "plaster of Paris" (a nearly ideal scatterer). The incident light was taken from

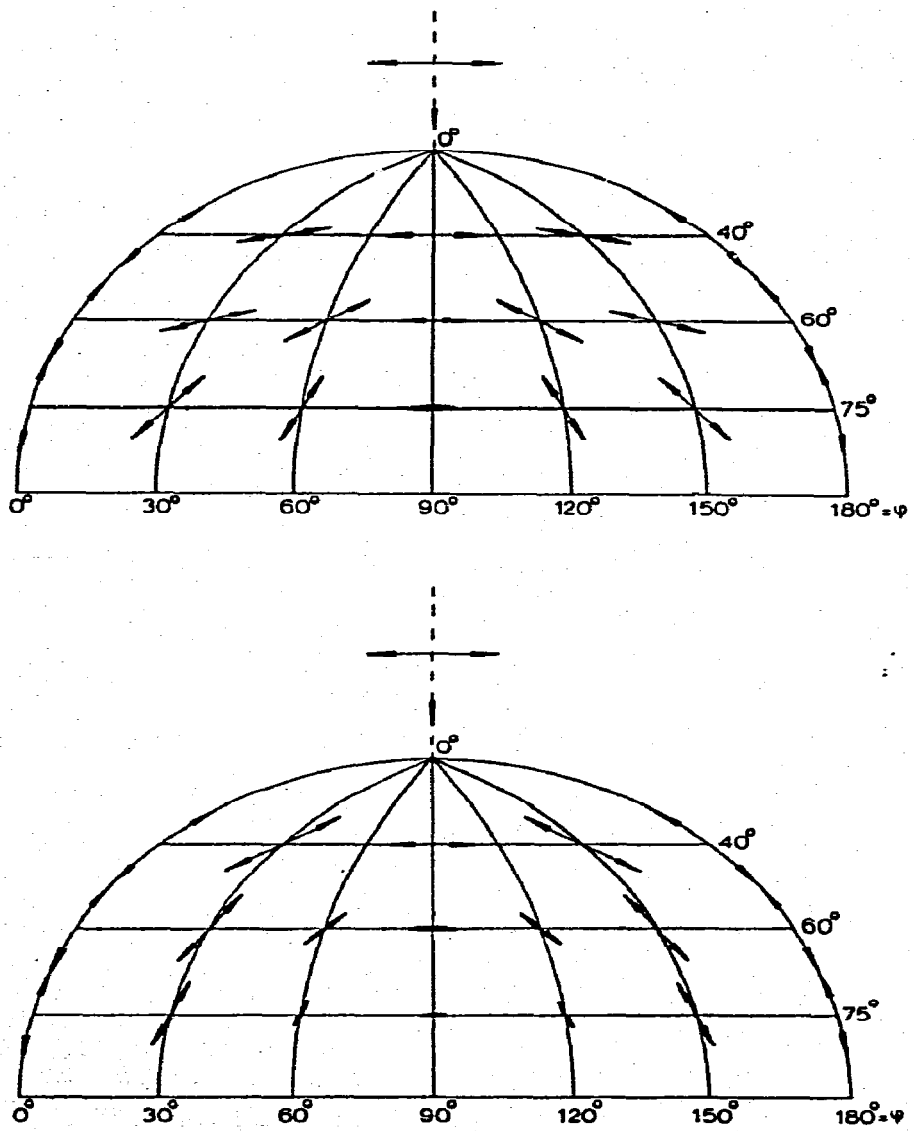

Figs. 3,4. (3) Experimental and (4) theoretical values of the relative intensity and angle of polarization of the light scattered by a mercury surface as a function of θ and φ. The incident beam is normal to the surface ($\theta_0 = 0$); its electrical component is in the plane of incidence. Data from ref. 12, by courtesy of Springer, Berlin.

the green region of the sunlight spectrum. The intensity from the mercury was 5.7×10^{-7} times the intensity from the plaster of Paris. Assuming that the plaster of Paris follows Lambert's law ($S = \cos\theta_0 \cos\theta/\pi$), then $S_{Hg} = 1.3 \times 10^{-7}$. The calculated value, obtained from the half sum of eqns. (3.17) and (3.19) using $\lambda_1 = 5400$ Å and $\gamma = 540$ dynes/cm, is $S_{Hg} = 1.5 \times 10^{-7}$. The agreement is reasonable.

4.1.2 Normal incidence ($\theta_0 = 0$); electrical component in plane of incidence

The (relative) intensity and the angle of polarization as a function of θ and φ were reported by Raman and Ramdas in the form of a diagram of which a redrawn version[12] is given in Fig. 3. The lengths of the arrows are proportional to S, their directions give the angle of polarization μ.

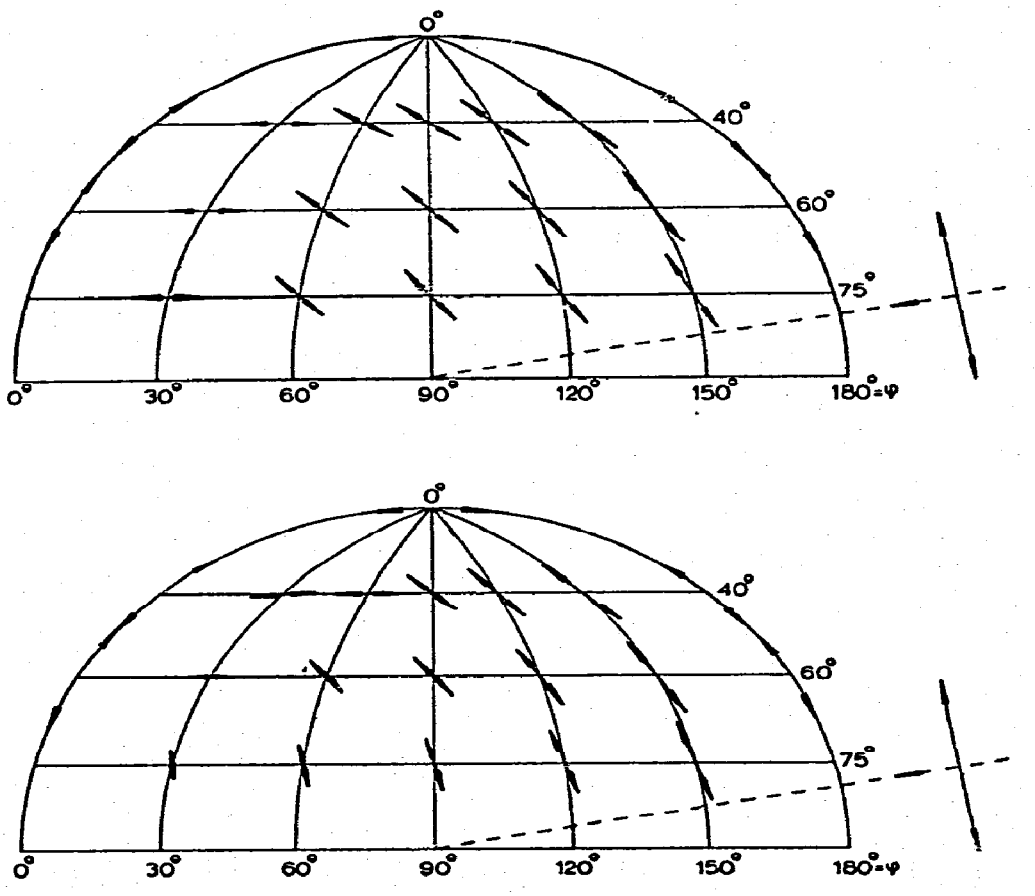

Figs. 5,6. (5) Experimental and (6) theoretical values of the relative intensity and angle of polarization of the light scattered by a mercury surface as a function of θ and φ. The incident light has a nearly-grazing angle of incidence ($\theta_0 = 80°$); its electrical component is in the plane of incidence.
Data from ref. 12, by courtesy of Springer, Berlin.

The diagram shows that the intensity is greatest in the azimuth containing the electric component of the incident light ($\varphi = 0°$ and $180°$) and smallest in perpendicular directions ($\varphi = 90°$ and $-90°$), which is just the opposite of what is normally encountered in the Rayleigh scattering of small particles.

The calculated[12] diagram is shown in Fig. 4.

4.1.3 Nearly grazing incidence ($\theta_0 = 80°$); electrical component in plane of incidence

Diagrams for the measured and calculated opalescence are given in Figs. 5 and 6. They show that generally more light is scattered in the forward (to the incident beam) than in the backward direction except near the reflected beam.

4.1.4 Discussion

The measured and calculated results are in qualitative agreement. The calculated angle dependence of the intensity, however, is much more pronounced than the experimental one. Raman and Ramdas state explicitly that both visual observation and photographic photometry do not show any increase in intensity when approaching the reflected beam. The discrepancy is clearly related to the factor $(\sin^2\theta_0 + \sin^2\theta - 2\sin\theta_0 \sin\theta \cos\varphi)$, present in all the light-scattering equations, due to the contribution of surface tension to the free energy of a corrugation. Raman[3] suggested that the surface opalescence exhibited by mercury may not be due to surface corrugations but to the mobility of the dispersion electrons assumed to exist in metals. This is supported by the fact that transparent liquids indeed show a steep increase in intensity when approaching the reflected or refracted beams.

It is difficult to see, however, why the absolute value of the measured intensity should be so close to the calculated one at medium angles (see 4.1.1).

Jagannathan[13] suggested that Mandelstam's statistical analysis of the corrugations is probably wrong, because the Fourier coefficients of the corrugations do not have the character of progressive waves but more of highly-damped aperiodic motions. This argument is not sound, however, because it is generally accepted that fluctuations near thermodynamic equilibrium may be calculated from the (equilibrium) free energy alone, which does not depend on the dynamics by which the fluctuation is created or annihilated. The dynamics of the fluctuation would be of importance only when explaining the *spectrum* of the surface opalescence (see section 1, small print).

It is also known from surface-tension measurements that it is very difficult to obtain a perfectly clean mercury surface.

More experimental data are needed before more definite conclusions can be reached.

4.2 SURFACE OF TRANSPARENT LIQUIDS

Experiments on the liquid–vapor interface were carried out by Raman and Ramdas[5,6]. The surfaces were made dust-free by repeated distillation *in vacuo* as described for mercury.

4.2.1 Qualitative observations

Sunlight was focussed on the surface of the liquid, half filling a spherical bulb. The surface opalescence observed varied strongly with the angles of incidence and observation, in contrast with the accompanying opalescence from the bulk. The color of the surface opalescence appeared much less blue than that of the bulk scattering, which is in accordance with the difference in wave dependence of the two phenomena. Observations of the intensity and polarization were reported for ethyl ether, which shows the surface opalescence strongly whilst its bulk opalescence is relatively small. One case will be described.

For unpolarized light falling in normally from above ($\theta_0 = 0$; $n > 1$), the surface opalescence was barely visible from above, but better from below, especially when $\theta' \approx 0°$. At larger θ' the intensity did not change markedly until the angle of total reflection was reached, $\theta' = \sin^{-1}(1/n)$, where it increased considerably. With further increase of θ' it decreased steadily. The scattering in the nearly-vertical direction was unpolarized. At the angle of total reflection the polarization was remarkably complete, with the electrical component parallel to the liquid surface; at still higher θ' the polarization became partial.

These observations may be expected from theory. For the intensity one obtains from the half sum of the eqns. (3.9) and (3.13) with $\theta_0 = \theta_0' = 0$; $t_{os}(1) = t_{op}(1)$:

$$S(2) = \tfrac{1}{2}nHt_{os}^2(1)[t_s^2(2) + t_p^2(2)\cos^2\theta] \tag{4.1}$$

Calculating $S(2)$ as a function of θ', using this equation, shows that it becomes maximal at the angle of total reflection [$\theta' = \sin^{-1}(1/n)$; $\theta = 90°$]. The factor $\cos^2\theta$ in eqn. (4.1) becomes zero at this angle, which means that only the electrical component parallel to the liquid surface remains. At $\theta' >$ angle of total reflection, the light becomes elliptically polarized.

4.2.2 Intensity of the surface opalescence of several liquids

The surface opalescence of a number of liquids was compared visually with water as a standard[5,6]. In this way, it is possible to determine whether the surface opalescence is proportional to the factor $(n^2 - 1)^2/\gamma$. If this is the case, the values in the last column of Table 1 (calculated by the author) should be constant. It is clear that the spread in S is greater than that in $S\gamma/100(n^2 - 1)^2$, but the constancy

TABLE 1

SURFACE SCATTERING OF TRANSPARENT LIQUIDS
(The values in the last column should theoretically be constant)

Substance	γ *(dynes/cm)*	n_F	S	$\frac{S\gamma}{100\,(n^2-1)^2}$
water	72	1.336	1	1.2
n-pentane	15.5	1.353	11.3	2.5
isopentane	14.5	1.352	8.9	1.9
hexane	16.3	1.374	8.5	1.8
heptane	20	1.387	8.8	2.0
octane	20	1.396	7.8	1.8
ethylene chloride	30	1.445	3.8	1.0
chloroform	25.3	1.446	6.3	1.4
carbon tetrachloride	24.6	1.462	12.6	2.4
silicon tetrachloride	15.8	1.420	7.4	1.1
formic acid	35.8	1.372	4.6	2.1
acetic acid	23.5	1.373	4.9	1.5
propionic acid	26.6	1.387	5.8	1.8
butyric acid	26.7	1.397	6.3	1.9
ethyl ether	15.3	1.352	7.4	1.6
methanol	23.0	1.329	4.0	1.6
ethanol	22.0	1.363	5.2	1.6
2-propanol	21.3	1.380	7.2	1.9
n-butanol	24.4	1.400	7.4	2.0
2-butanol	22.8	1.397	9.3	2.4
2-pentanol	23.2	1.419	7.8	1.8
benzyl alcohol	39.7	1.547	10.0	2.1
ethyl formate	22.0	1.359	5.2	1.6
propyl formate	22.2	1.379	7.4	2.1
propyl acetate	22.0	1.385	5.6	1.5
acetaldehyde	21	1.329	4.9	1.8
methyl ethyl ketone	25	1.378	5.3	1.6

of the last factor is rather poor. This is probably due to the low accuracy of the (visual) measurements and due to the fact that no corrections were made for the accompanying bulk scattering.

4.2.3 Angle dependence of the scattered light

Raman and Ramdas[5,9] and Hariharan[16] measured the angle-dependence of the light scattered into the liquid phase from a methanol surface at θ = angle of total reflection, by visual and photographic photometry respectively. Non-polarized light was used that approached the surface from the liquid side at $\theta_0 \simeq 40°$. The intensity of the scattered light from the liquid surface (with respect to that of the plaster of Paris surface) as a function of azimuth φ, is plotted in Fig. 7. The curve represents the surface opalescence calculated from theory. Hariharan's measurements were not absolute; the intensity at $\varphi = 0$ was chosen to fit the curve. The plot shows that the scattered light depends greatly on the azimuth φ; far more strongly than for mercury. There is, however, only qualitative

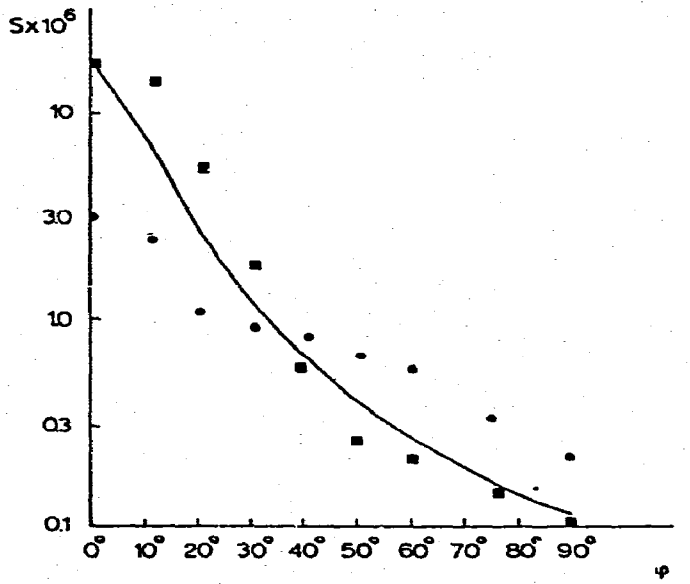

Fig. 7. Light scattering from a methanol surface as a function of φ. The curve is calculated from theory. (●) Experiments of Ramdas (visual photometry); (■) experiments of Hariharan (photographic photometry). The point of Hariharan at $\varphi = 0$ was chosen to fit on the curve.

agreement with the calculated curve — this is probably due to the low accuracy attained. Further, no corrections for the bulk light scattering were made.

Hariharan also measured the light scattered into the liquid phase, as a function of θ', when the incident light entered normally ($\theta_0 = 0$) from the vapor phase. He found a steep increase when the refracted beam was approached but not as steep as predicted by theory. The accuracy of his measurements, however, was too low to reach definite conclusions. We shall see later that the light scattering from a liquid film as a function of θ closely follows the theory (see section 5.2).

4.3 WATER SURFACES COVERED WITH FILMS

Raman and Ramdas[6,7] also made some observations on the light scattering from water surfaces covered with oleic acid and dye films. The surface opalescence increased about twofold when a water surface was covered with a quantity of oleic acid just sufficient to stop camphor movements. The scattered light was found to be less polarized. The opalescent spot on the surface was perfectly continuous. When, however, more oleic acid was used, the surface opalescence increased enormously and the opalescent spot, as seen in a microscope, was no longer continuous but showed a very large number of microscopic oil globules.

Water surfaces covered with (transient) dye films showed some interesting phenomena. Films of methyl violet produced a faint *yellowish-orange* surface opalescence (about the same tint as the light reflected by the surface of a dry crystal). The intensity was about 3 times that of a pure water surface. Films of tetraiodofluorescein, eosin, erythrosin, etc. showed intensely *green fluorescent* spots.

4.4 INTERFACES NEAR THE CRITICAL POINT

The surface opalescence of the liquid–vapor interface of carbon dioxide near the critical point was measured by Raman and Ramdas[6,8,9]. With unfiltered sunlight it could be seen very distinctly; it was much less blue and more intense than the bulk scattering.

As expected, the intensity increased enormously as the temperature approached the critical temperature (31.131°C). When the temperature was increased still further, the opalescent interface ceased to be sharp and extended over a certain thickness which increased with further increase in temperature until it filled the whole glass bulb at 31.377°C; at the same time the reflected beam vanished. The scattering above 31.131°C is probably a transition effect between pure surface scattering and bulk scattering. The intensity of the surface opalescence was measured as a function of temperature [red filter; $\theta_0 = 45°$; θ = critical angle (both from the liquid side)]. The results as given in Table 2 show that the agreement between theory and experiment is fair.

TABLE 2

LIGHT SCATTERING FROM THE LIQUID–VAPOR INTERFACE OF CARBON DIOXIDE AS A FUNCTION OF TEMPERATURE

t(°C)	*γ(dynes/cm)**	*S(CO₂ interface)/ S (Plaster of Paris)***		*S (observed)/ S (calculated)*
		(observed)	*(calculated)*	
31.10	0.00015	3000	3200	0.94
31.05	0.00060	1100	990	1.11
31.00	0.0012	500	600	0.83
30.80	0.0032	270	300	0.90
30.60	0.009	120	150	0.80
30.40	0.027	90	120	0.75
30.20	0.035	70	100	0.70
30.00	0.049	60	90	0.67

* Calculated values
** Plaster of Paris is a nearly ideal scatterer.

Barikhanskaya[14,15] investigated the dependence of surface opalescence on wavelength. The surface opalescence of a phenol–water and isobutyric acid–water interface was measured in a Koenig and Martens spectrophotometer near the critical solution temperatures. The logarithm of the opalescence was plotted *vs.* log λ. The slope of the line thus found changed from —3.2 to —2.1 in the temperature range 23.1–24.8°C (critical temperature). The slope should equal —2 according to theory. The discrepancy at the lower temperatures could be explained from the fact that the accompanying bulk scattering, which varies as λ^{-4}, increases much less with increasing temperature than the surface scattering so that it can be neglected at 24.8°C but not at 23.1°C.

5. Thin liquid films

The light scattering from thin free liquid films such as those found in soap bubbles was investigated by the author[21,25]. The interpretation of the surface scattering of a film is more complicated than it is for a single interface. Firstly, a free film has two interfaces and the interference of both the reflected and the scattered light waves has to be taken into account. Secondly, a stabilizing component, necessary to stabilize the film, is always present. Thirdly, internal forces, *e.g.* double-layer and van der Waals's forces between the two surfaces of the film, influence the corrugations of the surfaces and give rise to phase correlations between the corrugations of the two surfaces. The influence of internal interaction forces on the scattering opens the possibility of investigating these forces by measuring the light scattering, thus creating a new and fairly direct method of studying them quantitatively.

5.1 THEORY

The theory of Mandelstam (see section 3) was extended to a homogeneous film (medium 2) of mean thickness h_0 between two identical homogeneous media 1 and 3 (say air). The corrugations in the upper (1–2) and lower (2–3) interfaces are now given by[21]

$$\zeta = \Sigma \Sigma \zeta_{\varrho\sigma} \, e^{ip(\varrho x + \sigma y)} \tag{5.1}$$

$$\eta = \Sigma \Sigma \eta_{\varrho\sigma} \, e^{ip(\varrho x + \sigma y)} \tag{5.2}$$

and the increase in free energy of the corrugated film now becomes, if the influence of gravity is neglected,

$$\Delta F = \Delta F_1 + \Delta F_3 \tag{5.3}$$

where

$$\Delta F_1 = \tfrac{1}{2}\gamma \iint \left(\frac{\delta\zeta}{\delta x}\right)^2 + \left(\frac{\delta\zeta}{\delta y}\right)^2 + \left(\frac{\delta\eta}{\delta x}\right)^2 + \left(\frac{\delta\eta}{\delta y}\right)^2 \Big] \, dx \, dy \tag{5.4}$$

and

$$\Delta F_3 = \tfrac{1}{2}\left(\frac{d^2V}{dh^2}\right)_0 \iint (\zeta - \eta)^2 \, dx \, dy \tag{5.5}$$

ΔF_3 contains the thickness fluctuation $(\zeta - \eta)$ of the film and the second derivative of that part of the free energy of the film that depends on its thickness because of intermolecular interactions.

For further analysis it was convenient to split ΔF as follows

$$\Delta F = \Delta F' + \Delta F'' \tag{5.6}$$

where

$$\Delta F' = \tfrac{1}{4}\gamma \iint \{(\delta(\zeta + \eta)/\delta x)^2 + (\delta(\zeta + \eta)/\delta y)^2\}\, dx\, dy \tag{5.7}$$

and

$$\Delta F'' = \iint \{\tfrac{1}{4}\gamma[(\delta(\zeta - \eta)/\delta x)^2 + (\delta(\zeta - \eta)/\delta y)^2] + \tfrac{1}{2}V''(\zeta - \eta)^2\}\, dx\, dy \tag{5.8}$$

The corrugations of the two single interfaces ζ and η, are now replaced by "normal" corrugations given by the linear combinations $(\zeta + \eta)$ and $(\zeta - \eta)$. Thus $\Delta F'$ is associated with fluctuations in the bending of the film as a whole and $\Delta F''$ is associated with fluctuations in the film thickness.

The mean square Fourier coefficients needed for the calculation of the light scattering now become:

$$\overline{(\zeta_{\varrho\sigma} + \eta_{\varrho\sigma})\,(\zeta_{\varrho\sigma} + \eta_{\varrho\sigma})^*} = \frac{2kT}{\gamma a^2 p^2 (\varrho^2 + \sigma^2)} \tag{5.9}$$

and

$$\overline{(\zeta_{\varrho\sigma} - \eta_{\varrho\sigma})\,(\zeta_{\varrho\sigma} - \eta_{\varrho\sigma})^*} = \frac{2kT}{\gamma a^2 p^2 (\varrho^2 + \sigma^2) + 2a^2 \dfrac{d^2V}{dh^2}} \tag{5.10}$$

Cross products of the form $\overline{(\zeta_{\varrho\sigma} + \eta_{\varrho\sigma})\,(\zeta_{\varrho\sigma} - \eta_{\varrho\sigma})^*}$ are zero because of the relations

$$\overline{\zeta\zeta^*} = \overline{\eta\eta^*}; \quad \overline{\zeta\eta^*} = \overline{\zeta^*\eta}.$$

The amplitude for the scattered light is a linear function of $\zeta_{\varrho\sigma}$ and $\eta_{\varrho\sigma}$ and can be written as follows:

$$A_{\varrho\sigma} = \tfrac{1}{2}(M + N)\,(\zeta_{\varrho\sigma} + \eta_{\varrho\sigma}) + \tfrac{1}{2}(M - N)\,(\zeta_{\varrho\sigma} - \eta_{\varrho\sigma}) \tag{5.11}$$

For incident light polarized with the electrical component *normal* to the plane of incidence (XZ-plane) and for scattering observed in the same plane, on the *reflection* side of the film it was found that:

$$\begin{aligned} M &= L(1 - r_0\, e^{-2i\beta})\,(1 - r e^{-2i\alpha}) \\ N &= -L t_{0s}(2)\, t_s(2)\, e^{-i\beta}\, e^{-i\alpha} \end{aligned} \tag{5.12}$$

where

$$L = [i\pi(n^2 - 1)\, t_{0s}(1)\, t_s(1)/\lambda_1 \cos\theta]\,[(1 - r_0^2\, e^{-2i\beta})\,(1 - r^2\, e^{-2i\alpha})]^{-1} \tag{5.13}$$

With

$$r_0 = t_{0s}(1) - 1; \quad r = t_s(1) - 1; \quad t_{0s}(2) = 2 - t_{0s}(1) \tag{5.14}$$

The t-coefficients were defined above (eqns. 3.1–3.3); $\alpha = 2\pi n h \cos\theta'/\lambda_1$; $\beta = 2\pi n h \cos\theta_0'/\lambda_1$; h = film thickness.

The intensity of the scattering, on the reflection side of the film, becomes ($\varphi = 0$)

$$S^R = A + \tfrac{1}{2}H\{G_0 G_3 + [G_0(2G_1 - G_3)]\,[1 + (2Q/\gamma)\,(\sin\theta - \sin\theta_0)^{-2}]^{-1}\} \tag{5.15}$$

where A is the residual bulk scattering and H is defined by eqn. (3.5).

$$G_0 = t_s^2(1)\ t_{0s}^2(1)\ [R(r^2,\ a)\ R(r_0^2,\ \beta)]^{-1} \tag{5.16}$$

$$G_1 = R(r,\ a)\ R(r_0,\ \beta) + t_s^2(2)\ t_{os}^2(2) \tag{5.17}$$

$$G_2 = R(r_0,\ \beta)\ t_s^2(2) + R(r,a)\ t_{os}^2(2) \tag{5.18}$$

$$G_3 = G_1 - 2t_s^2(2)\ t_{os}^2(2)\ \cos\alpha\ \cos\beta + 2t_s(1)\ t_s(2)\ t_{os}(1)\ t_{os}(2)\ \sin\alpha\ \sin\beta \tag{5.19}$$

$$R(r,\ a) = 1 + r^2 - 2r\ \cos 2a \tag{5.20}$$

$$R(r_0,\ \beta) = 1 + r_0^2 - 2r_0\ \cos 2\beta \tag{5.21}$$

$$R(r^2,\ a) = 1 + r^4 - 2r^2\ \cos 2a \tag{5.22}$$

$$R(r_0^2,\ \beta) = 1 + r_0^4 - 2r_0^2\ \cos 2\beta \tag{5.23}$$

$$Q = (\lambda_1^2/4\pi^2)\ (d^2V/dh^2) \tag{5.24}$$

The function $Q(h)$ is a consequence of the intermolecular interactions in the film, whereas the G-functions are a consequence of the optical complications due to interference of the light.

The first term in the brackets of eqn. (5.15), G_0G_3, originates from fluctuations in $(\zeta + \eta)$ and the second term from fluctuations in $(\zeta - \eta)$. G_0G_3 predominates when $2Q \gg \gamma(\sin\theta - \sin\theta_0)^2$, i.e. when the free energy of two opposite film elements depends largely on the distance of separation and far less on the increase in surface area. When $2Q \ll \gamma(\sin\theta - \sin\theta_0)^2$, the sum of both terms in the brackets reduces to $2G_0G_1$, so that, respectively:

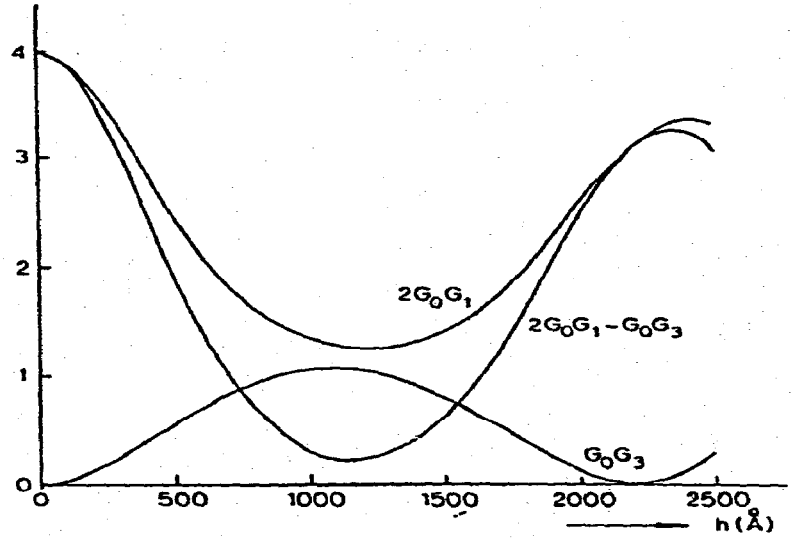

Fig. 8. Intensity of the light scattered from fluctuations in $(\zeta + \eta)$:G_0G_3, and from fluctuations in $(\zeta - \eta)$:$(2G_0G_1 - G_0G_3)$. When the intermolecular forces are small the intensity approaches $2G_0G_1$ ($\theta_0 = 60°$; $n = 1.36$; $\lambda_1 = 5460$ Å).

$$S^R = A + (H/2)G_0G_3 \tag{5.25}$$

for thin films, and

$$S^R = A + H\,G_0G_1 \tag{5.26}$$

for thick films.

The G-functions are oscillating functions of h (through α, β) (see Fig. 8). G_0G_3 shows a similar dependence on h as the *regular reflection* $|r|^2$; its maxima and minima alternate with those of G_0G_1. It was indeed found experimentally that the maxima and minima in the light scattering of a rather thick film, where Q is expected to be small, alternate with those of the regular reflection.

5.2 EXPERIMENTS

Experiments were carried out by the author[21] on films drawn from a solution containing 0.64 g OP7 (octylphenol condensed with about 7 ethylene oxide molecules), 0.0087 g sodium lauryl sulfate, 20 ml glycerol, and water up to a volume of 100 ml. The refractive indices of the solution at 5460 Å and 4360 Å were 1.360 and 1.365, respectively; the surface tension was 33 dynes/cm. The soap film was suspended on a rectangular glass frame inside a closed light-scattering cell. The light scattering from the film was measured with a photomultiplier at $\theta = 0 \rightarrow 44°$ in the plane of the incident light ($\varphi = 0$). The incident light beam was polarized with its electrical component parallel to the film surface, with angle

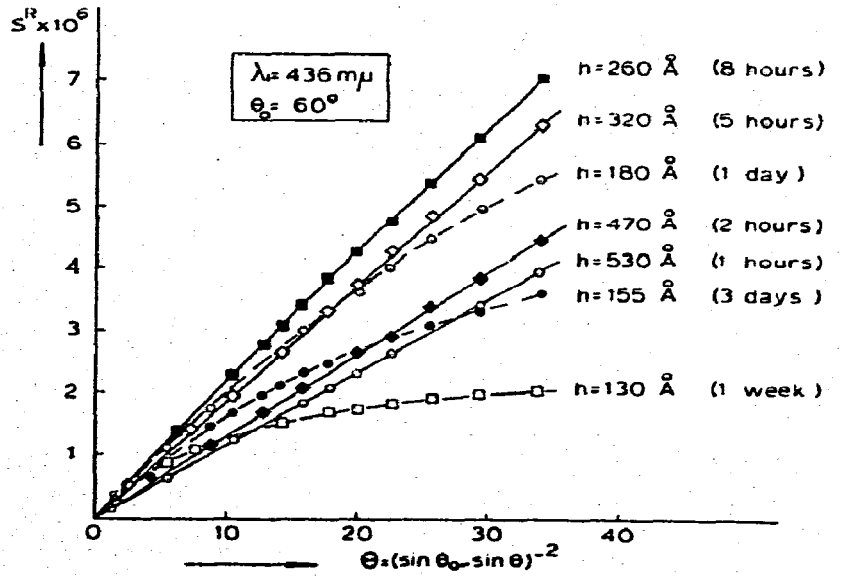

Fig. 9. Light scattering of a free soap film as a function of $\Theta = (\sin\theta_0 - \sin\theta)^{-2}$ at various thicknesses and drainage times. Several points near the origin are omitted for clarity. Data from ref. 21, by courtesy of Academic Press, Inc., New York.

of incidence $\theta_0 = 60°$. The apparatus was calibrated with a MgO diffusor (accuracy not better than 10 %). The thickness of the film was obtained from the intensity of the light reflected by the film.

In Fig. 9 the scattering intensity, S^R, is plotted as a function of $\Theta = (\sin\theta_0 - \sin\theta)^{-2}$, at various film thicknesses, h. For $h = 530$-320 Å, the plots are proportional to Θ; A is negligible.

Eqns. (5.25) and (5.26) are both linear in Θ (through H) but from the fact that the slope of the S^R *vs.* Θ plot increases with decreasing h, it may be concluded that eqn. (5.26) applies because G_0G_1 increases with h, but G_0G_3 decreases with h in the range of h considered. Thus Q is small for $h = 530$-320 Å. For smaller h, the plot S^R *vs.* Θ is no longer linear; this may be explained by an increase of Q.

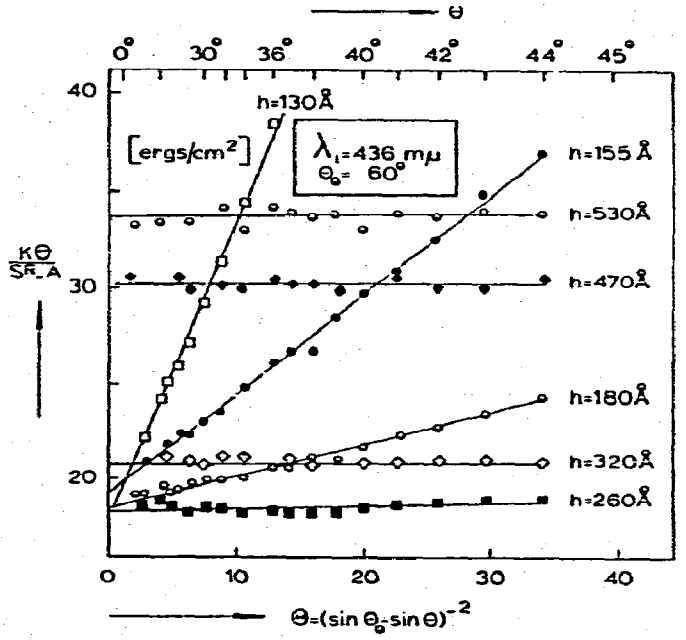

Fig. 10. Reduced light scattering of a free soap film as a function of $\Theta = (\sin\theta_0 - \sin\theta)^{-2}$ at various thicknesses. The line for $h = 130$ Å remains linear up to $\Theta = 35$. Data from ref. 21, by courtesy of Academic Press, Inc., New York.

γ and Q were obtained by plotting $K\Theta/(S^R - A)$ *vs.* Θ (see Fig. 10); $K = (n^2 - 1)^2\,(kT/4\lambda_1^2)$ and, using the following equation obtained from eqn. (5.15) by series expansion:

$$\frac{K\Theta}{S^R - A} = \frac{\gamma}{G_0G_1} + \frac{(2 - \chi)\,Q\Theta}{G_0G_1} + \ldots \qquad (5.27)$$

where $\chi = G_3/G_1$. This equation applies when $Q < (\gamma/\chi\Theta)$. The function G_0G_1 does not depend very much on θ. The values of γ, Q and (d^2V/dh^2) given in Table 3 were calculated from the intercept and slope of Fig. 10.

TABLE 3

SURFACE TENSION, γ, AND SECOND DERIVATIVE OF FREE ENERGY (d^2V/dh^2) OF FREE SOAP FILM OBTAINED FROM LIGHT-SCATTERING DATA[25]

λ_1 (Å)	h (Å)	$\frac{\gamma}{G_0G_1}$	γ (dynes/cm)	$\frac{(2-\chi)Q}{G_0G_1}$	Q	$\frac{d^2V}{dh^2} \times 10^{-10}$ (ergs cm^{-4})
5460	130	19	36.5	2.20	2.15	2.85
4360	130	18.5	35	1.50	1.45	3.00
5460	155	19.5	37	0.76	0.74	0.98
4360	155	19.5	36	0.52	0.49	1.02
4360	180	18.5	33.5	0.17	0.16	0.33
5460	190	17.5	32	0.19	0.18	0.24
4360	260	18.5	29.5	0.02	0.015	0.03
5460	320	18	29			
4360	320	21	30			
4360	470	30	32.5			
5460	505	24.5	30.5			
4360	530	34	33			
5460	670	32	31			

The values of γ thus found show some scatter but the mean values 32.6 at $\lambda_1 = 5460$ Å and 32.8 at $\lambda_1 = 4360$ Å are in agreement, thus supporting the λ^2 dependence of S. They are also in agreement with the surface tension of the solution (33 dynes/cm). The values of d^2V/dh^2 at both wavelengths are also in satisfactory agreement, which confirms the λ^2 dependence of Q.

Further, no indications were found of a deviation of S^R from the dependence on $\Theta = (\sin\theta_0 - \sin\theta)^{-2}$ as had been found by previous authors (see section 4).

5.3 INTERACTION BETWEEN THE FILM SURFACES

The values of d^2V/dh^2 found above were compared with calculated values using the following model, discussed by Overbeek[26]. The film is composed of a bulk layer of soap solution covered with adsorbed soap ions. The contribution to the free energy of electrostatic repulsion between the film surfaces is

$$V = B\varkappa\, e^{-\varkappa h} \tag{5.28}$$

where $B = 8\varepsilon k^2T^2\Phi^2/\pi e^2 = 1.47 \times 10^{-6}\Phi^2$; k = Boltzmann's constant; $\varkappa = (8\pi ne^2/\varepsilon kT)^{\frac{1}{2}}$; $\Phi = \tanh(e\psi_0/4kT)$; ψ_0 = surface potential; h = film thickness. The second derivative of V is

$$\frac{d^2V}{dh^2} = B\varkappa^3\, e^{-\varkappa h} \tag{5.29}$$

According to this equation a plot of $\log(d^2V/dh^2)$ should be linear in h. Fig. 11 shows that this is indeed the case.

From the slope and intercept of this plot the values $\varkappa = 4.2 \times 10^6$ cm^{-1};

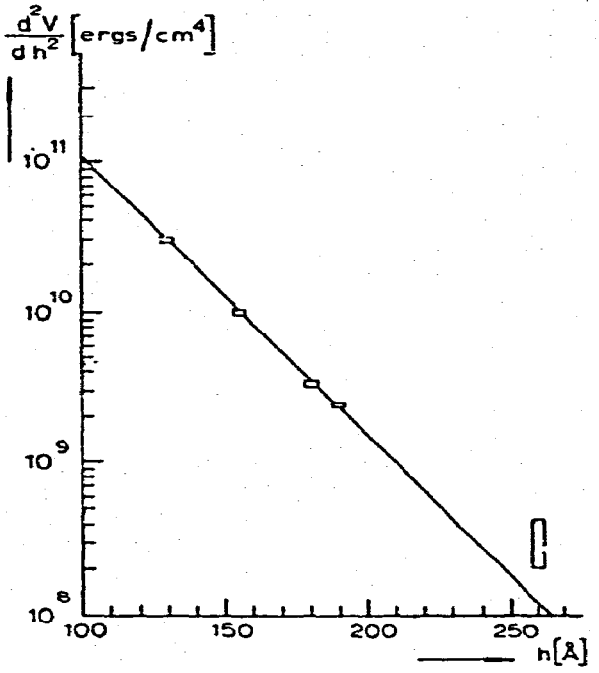

Fig. 11. Interaction between film surfaces as a function of thickness. Data from ref. 21, by courtesy of Academic Press, Inc., New York.

$B = 9.3 \times 10^{-8}$ and $\psi_0 = 25$ mV were obtained. However, the $\varkappa$-value thus found is about 4 times higher than would be expected from the conductance of the soap solution. Inclusion of van der Waals' attraction forces in V somewhat increases ψ_0 and decreases $\varkappa$. Part of the discrepancy may be due to some evaporation of the film.

The experiments on soap films reported above were only preliminary; we hope to report more systematic measurements in the future. We shall also investigate whether the sandwich structure of the soap film introduces a significant correction in the light scattering equations.

ACKNOWLEDGEMENT

The author thanks Professor J. T. G. Overbeek for his critical study of the manuscript and for his advice.

References

1 M. VON SCHMOLUCHOWSKI, *Ann. Physik*, 25 (1908) 225.
2 L. MANDELSTAM, *Ann. Physik*, 41 (1913) 609.
3 C. V. RAMAN, *Nature*, 112 (1923) 281.
4 C. V. RAMAN AND L. A. RAMDAS, *Proc. Roy. Soc. (London), Ser. A*, 108 (1925) 561.

5 C. V. RAMAN AND L. A. RAMDAS, *Proc. Roy. Soc. (London), Ser. A*, 109 (1925) 150.
6 C. V. RAMAN AND L. A. RAMDAS, *Proc. Roy. Soc. (London), Ser. A*, 109 (1925) 272.
7 L. A. RAMDAS, *Indian J. Phys.*, 1 (1927) 29.
8 C. V. RAMAN, *Indian J. Phys.*, 1 (1927) 97.
9 L. A. RAMDAS, *Indian J. Phys.*, 1 (1927) 199.
10 R. GANS, *Ann. Physik*, 74 (1924) 231.
11 R. GANS, *Ann. Physik*, 79 (1926) 204.
12 A. ANDRONOV AND M. LEONTOVICZ, *Z. Physik*, 38 (1926) 485.
13 S. JAGANNATHAN, *Proc. Indian Acad. Sci.*, A1 (1934) 115.
14 F. BARIKHANSKAYA, *Phys. Z. Soviet Union*, 10 (1936) 666.
15 F. BARIKHANSKAYA, *J. Exptl. Theoret. Phys. USSR*, 7 (1937) 51.
16 P. S. HARIHARAN, *Proc. Indian Acad. Sci.*, A16 (1942) 290.
17 G. B. BENEDIK, J. B. LASTOVKA, K. FRITSCH AND T. GREYTAK, *J. Opt. Soc. Am.*, 54 (1964) 1284.
18 H. Z. CUMMINS, N. KNABLE AND Y. YEH, *Phys. Rev. Letters*, 12 (1964) 150.
19 D. H. RANK, E. M. KIESS, U. FINK AND T. A. WIGGINS, *J. Opt. Soc. Am.*, 55 (1965) 925.
20 S. S. ALPERT, Y. YEH AND E. LIPWORTH, *Phys. Rev. Letters*, 13 (1965) 486.
21 A. VRIJ, *J. Colloid Sci.*, 19 (1964) 1.
22 P. BECKMANN AND A. SPIZZICHINO, *The Scattering of Electromagnetic Waves from Rough Surfaces*, Pergamon Press, Oxford, 1963.
23 Lord RAYLEIGH, *Proc. Roy. Soc. (London), Ser. A*, 79 (1907) 399; *Scientific Papers*, Cambridge University Press, 1912, Vol. 5, p. 398.
24 M. BORN AND E. WOLF, *Principles of Optics*, Pergamon Press, London, 1959, p. 39.
25 A. VRIJ, *Proceedings of the 4th International Congress on Surface Activity, Brussels, 1964*, Gordon and Breach, London, 1967.
26 J. T. G. OVERBEEK, *J. Phys. Chem.*, 64 (1960) 1178.